

Photolysis of oxalyl chloride (CICO) 2 at 193 nm: Emission of CO (v6,J60) detected with time-resolved Fourier-transform spectroscopy

Chia-Yan Wu, Yuan-Pern Lee, and Niann S. Wang

Citation: *The Journal of Chemical Physics* **120**, 6957 (2004); doi: 10.1063/1.1669390

View online: <http://dx.doi.org/10.1063/1.1669390>

View Table of Contents: <http://scitation.aip.org/content/aip/journal/jcp/120/15?ver=pdfcov>

Published by the [AIP Publishing](#)

Articles you may be interested in

[Photodissociation dynamics of Cl N 3 at 193 nm](#)

J. Chem. Phys. **125**, 224304 (2006); 10.1063/1.2400854

[The lowest 1\(3 P J \) and 2\(3 P 2 \) ion-pair states of ClF: Nonadiabatic effects and emission spectra](#)

J. Chem. Phys. **117**, 628 (2002); 10.1063/1.1482371

[Short-wavelength photolysis of jet-cooled OCIO \(2 A 2 1 >20 \) CIO \(X 2 ,v,J\)+ O \(3 P J \)](#)

J. Chem. Phys. **114**, 8339 (2001); 10.1063/1.1367393

[Completely inverted ClO vibrational distribution from OCIO \(2 A 2 24,0,0 \)](#)

J. Chem. Phys. **112**, 5298 (2000); 10.1063/1.481100

[The rotational spectrum of chloryl chloride, ClCIO 2 , in its ground vibrational state](#)

J. Chem. Phys. **110**, 11865 (1999); 10.1063/1.479179



Re-register for Table of Content Alerts

Create a profile.



Sign up today!



Photolysis of oxalyl chloride $(\text{CICO})_2$ at 193 nm: Emission of CO ($v \leq 6$, $J \leq 60$) detected with time-resolved Fourier-transform spectroscopy

Chia-Yan Wu and Yuan-Pern Lee^{a)}

Department of Chemistry, National Tsing Hua University, 101, Sec. 2, Kuang Fu Road, Hsinchu 30013, Taiwan

Niann S. Wang

Department of Applied Chemistry, National Chiao Tung University, 1001, Ta Hsueh Road, Hsinchu 30010, Taiwan

(Received 12 November 2003; accepted 21 January 2004)

Upon photolysis of oxalyl chloride at 193 nm, time-resolved and rotationally resolved emission of CO ($v \leq 6$, $J \leq 60$) in the spectral region 1850–2350 cm^{-1} was detected with a step-scan Fourier-transform spectrometer under nearly collisionless conditions. Boltzmann-type rotational distributions of CO correspond to temperatures 3520 ± 110 ($v = 1$) to 2300 ± 610 K ($v = 6$), with an average rotational energy of 23 ± 2 kJ mol^{-1} . The average vibrational energy of CO is estimated to be 26 ± 4 kJ mol^{-1} according to observed vibrational populations of $v = 1-6$ and that of $v = 0$ predicted with a surprisal analysis. Combining the average internal energy of CO determined in this work and average translational energies of photofragments Cl and CO determined previously by Hemmi and Suits, we propose a four-body dissociation mechanism producing one pair of translationally rapid and internally excited CO and one pair of translationally rapid Cl, each with similar energies, to account for the energy balance. Formation of translationally slow CICO, Cl, and CO reported previously by Hemmi and Suits might be rationalized with a second channel involving emission of electronically excited intermediates. We observed no emission of CICO near 1880 cm^{-1} , indicating that surviving CICO has little vibrational excitation in the C–O stretching mode.

© 2004 American Institute of Physics. [DOI: 10.1063/1.1669390]

I. INTRODUCTION

Oxalyl chloride, $(\text{CICO})_2$, is an excellent source of chlorine atoms for laboratory experiments because of its large cross section for absorption in the ultraviolet (UV) region, and because it photodissociates into mainly Cl and CO, with the advantage of CO being unreactive.¹ Earlier investigations on $(\text{CICO})_2$ were briefly reviewed in our previous paper that describes our work on the dynamics studies of $(\text{CICO})_2$ upon photolysis at 248 nm using a step-scan Fourier-transform infrared (FTIR) spectrometer.²

Ahmed *et al.* investigated photodissociation dynamics of $(\text{CICO})_2$ near 235 nm with a photofragment imaging technique using resonance-enhanced multiphoton-ionization (REMPI) detection of Cl and CO.³ Images of photofragments $\text{Cl}^*(^2P_{1/2})$, $\text{Cl}(^2P_{3/2})$, and $\text{CO}(v = 0)$ in various rotational levels were recorded to yield distributions of their translational energy. The distribution of recoil speed of Cl^* exhibits a dominant component with a distribution of translational energy peaking ~ 48 kJ mol^{-1} , whereas that of Cl shows two components with a dominant component peaking ~ 10 kJ mol^{-1} and a minor component similar to Cl^* . These translationally rapid components of both Cl and Cl^* , and the higher rotational levels of CO, show anisotropic angular distributions, whereas the slow fragments exhibit nearly isotropic distributions. The reported rotational distribution of

$\text{CO}(v = 0)$, upon photolysis at 235 nm, shows $J_{\text{max}} = 50$ and a maximal population near $J = 30$.³ Using a step-scan FTIR spectrometer to study photolysis of $(\text{CICO})_2$ at 248 nm,² we observed rotational distributions of $\text{CO}(v = 1, 2)$ with rotational temperatures $\sim 20\%$ greater than that reported for $\text{CO}(v = 0)$ by Ahmed *et al.*³ The discrepancy might result from a contribution of rotationally cold CO in the $v = 0$ state in their experiments; these cold CO molecules are produced from secondary dissociation of chloroformyl radical (CICO) product. These authors reported that the total integrated intensity of the (1–1) band of CO was less than 5% that of the (0–0) band in their REMPI spectra.³ Our results indicated more vibrational excitation of CO, with v up to 3 being populated. The discrepancy might be due to the predissociative character of intermediate states of $\text{CO}(v > 1)$ before ionization in the REMPI scheme; a significant portion of vibrationally excited CO might have escaped detection.

Ahmed *et al.*³ suggested that photodissociation of $(\text{CICO})_2$ proceeds via an impulsive three-body mechanism yielding translationally rapid Cl^* and Cl, translationally rapid and rotationally excited CO, and translationally slow CICO; most CICO undergoes subsequent dissociation to yield two translationally slow species: CO with little rotational energy and Cl. Based on their experimental results, Ahmed *et al.* derived an average total energy release on photodissociation of $(\text{CICO})_2$ at 235 nm ~ 26 kJ mol^{-1} greater than the available energy calculated from corresponding enthalpies of formation. We combined the internal energy of

^{a)} Author to whom correspondence should be addressed. Fax: 886-3-5722892. Electronic mail: yplee@mx.nthu.edu.tw

CO determined in our work² with translational energies determined previously^{3,4} to derive a revised energy balance that fits satisfactorily with the proposed two-step dissociation mechanism for photodissociation of $(\text{ClCO})_2$ at 248 nm.

Hemmi and Suits⁴ also investigated photodissociation of $(\text{ClCO})_2$ at 193 nm with photofragment translational spectroscopy by employing for ionization the tunable VUV light from a synchrotron. They reported that distributions of translational energy of both Cl and CO are bimodal and are similar to those observed at 235 nm, whereas the distribution for ClCO has a single sharp maximum with an abrupt lack of population for translational energies less than $\sim 4 \text{ kJ mol}^{-1}$, confirming that highly internally excited, hence translationally cold, ClCO product undergoes secondary dissociation to form Cl and CO.³ Because observed translational energies of fragments are similar at both photolysis wavelengths, the additional energy of 110 kJ mol^{-1} in switching from 235 to 193 nm for photolysis is expected to be distributed to the internal degree of freedom of CO. The internal energy of CO produced upon photolysis at 193 nm was not determined in previous work.

In this paper we report observation of IR emission of $\text{CO}(v \leq 6)$ with time-resolve Fourier-transform spectroscopy (TR-FTS) upon photolysis of $(\text{ClCO})_2$ at 193 nm; a four-body mechanism of decomposition is proposed to account for the energy balance.

II. EXPERIMENT

The apparatus employed to obtain time-resolved infrared emission spectra has been described previously;^{2,5,6} only a summary is given here. The photolysis beam from an ArF laser (193 nm, Lambda Physik, Optex) has dimensions $\sim 4 \times 8 \text{ mm}^2$ with output energy $\sim 7 \text{ mJ}$ per pulse. A filter (OCLI, W05200-6X) passing $1670\text{--}2325 \text{ cm}^{-1}$ was employed to facilitate undersampling to decrease the number of data points; 5034 scan steps were performed to yield an interferogram resulting in a CO emission spectrum with a resolution of 0.13 cm^{-1} . Data were averaged over 70 laser pulses at each scan step. The InSb detector system has a rise time $\sim 0.7 \mu\text{s}$; its signal was further amplified with an effective bandwidth of 1 MHz before being digitized with an external data-acquisition board (PAD1232, 12-bit ADC) at 50-ns intervals. Time-resolved spectra at 50-ns intervals were typically summed over periods of $0.5 \mu\text{s}$ after photolysis to yield spectra with a signal-to-noise ratio suitable for quantitative analysis.

$(\text{ClCO})_2$ (Lancaster, $>98\%$) was used without purification except for degassing at 77 K. The pressure of $(\text{ClCO})_2$ in the flow cell was kept below 0.035 Torr and no buffer gas was added.

III. RESULTS AND DISCUSSION

We employed a total pressure of 0.035 Torr to maintain nearly collisionless conditions within $\sim 1.5 \mu\text{s}$ period after photolysis. The absorption cross section of $(\text{ClCO})_2$ at 193 nm is $\sim 3.8 \times 10^{-18} \text{ cm}^2$;¹ hence about 8% of $(\text{ClCO})_2$ was dissociated upon irradiation. Spectra of improved ratio of

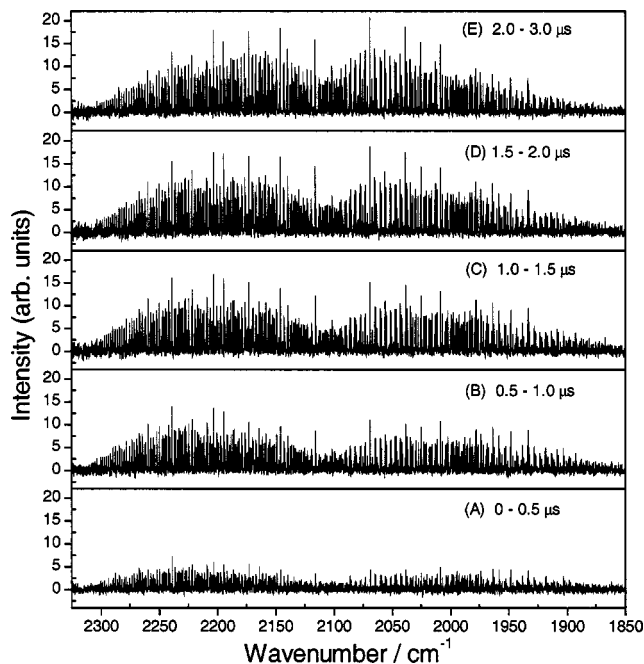


FIG. 1. Infrared emission spectra of CO in the spectral region $2350\text{--}1850 \text{ cm}^{-1}$ averaged for periods $0\text{--}0.5 \mu\text{s}$ (A), $0.5\text{--}1.0 \mu\text{s}$ (B), $1.0\text{--}1.5 \mu\text{s}$ (C), $1.5\text{--}2.0 \mu\text{s}$ (D), and $2.0\text{--}3.0 \mu\text{s}$ (E) after photolysis of $(\text{ClCO})_2$ at 0.035 Torr and 298 K with an ArF laser at 193 nm. Resolution is 0.13 cm^{-1} ; 70 laser pulses were averaged at each scan step. Six spectra recorded under similar conditions were averaged.

signal to noise were obtained on averaging six sets of spectra recorded in separate experiments under similar conditions.

A. Spectral assignments and rotational distribution of CO

Figure 1 shows emission spectra of CO at 0.13 cm^{-1} resolution and averaged over $0\text{--}0.5$, $0.5\text{--}1.0$, $1.0\text{--}1.5$, $1.5\text{--}2.0$, and $2.0\text{--}3.0 \mu\text{s}$ after laser irradiation of $(\text{ClCO})_2$ at 0.035 Torr. The small intensity in Figs. 1(A) and 1(B) reflects the slow response of the amplification system $\sim 1 \mu\text{s}$. Rotational quenching becomes perceptible after $\sim 1.5 \mu\text{s}$, as shown in Figs. 1(D) and 1(E). To show clearly rotational bands in each vibrational state, an expanded spectrum averaged over $0\text{--}1.5 \mu\text{s}$ is shown in Fig. 2. The assignments based on spectral parameters reported by Ogilvie *et al.*⁷ are marked as sticks; rotational quantum numbers (J'') of the lower states for each $(v' - v'')$ transition are indicated. Emission lines from rotational levels of CO with J' up to 55 (P branch) or 60 (R branch) were observed. The spectrum demonstrates that the resolution of 0.13 cm^{-1} is adequate to resolve most lines for $v' = 1\text{--}6$.

We calculated values of the Einstein A coefficient as described previously;² Einstein coefficients calculated for large values of J and v are expected to be reasonably reliable because the function for dipolar moment employed in the calculations shows satisfactory agreement with results from quantum-chemical computations well beyond its range of definition from experiment. Each vibration-rotational line was normalized with the instrumental response function, integrated, and divided by its respective Einstein coefficient to yield a relative population $P_v(J')$. To assess the effect of

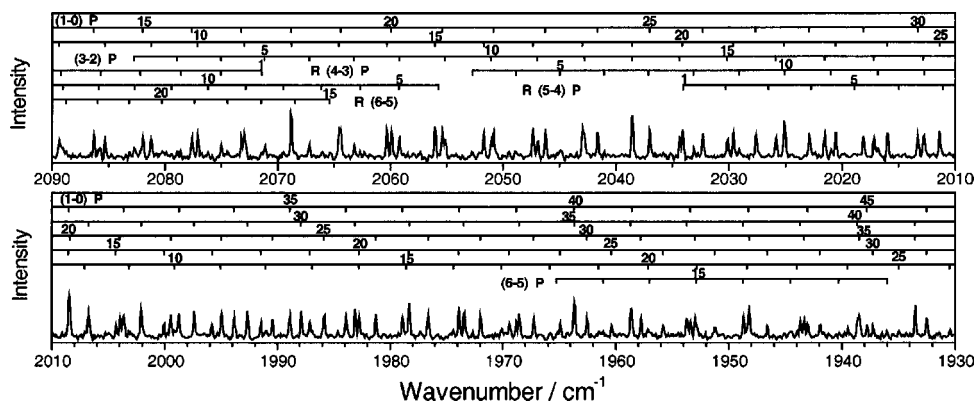


FIG. 2. Partial infrared emission spectra of CO in the spectral region 2090–1930 cm^{-1} averaged for 0–1.5 μs after photolysis of $(\text{CICO})_2$ at 0.035 Torr and 298 K with laser light at 193 nm. Assignments are shown in stick diagrams.

rotational quenching, we made semilogarithmic plots of $P_v(J')/(2J'+1)$ of $\text{CO}(v=1)$ for spectra obtained with integration periods 0–0.5, 0.5–1.0, 1.0–1.5, and 1.5–2.0 μs , and found Boltzmann-type rotational distributions corresponding to rotational temperatures of 3710 ± 320 , 3590 ± 150 , 3410 ± 100 , and 3020 ± 80 K, respectively; the uncertainties reflect one standard deviation in fitting. Considering possible experimental errors, we conclude that rotational quenching is negligible within 1.5 μs . Hence we used spectra integrated over 0–1.5 μs for measurements of the nascent distribution. Semilogarithmic plots of $P_v(J')/(2J'+1)$ vs $J'(J'+1)$ for P and R branches of $\text{CO}(v=1-6)$ recorded for period 0–1.5 μs are shown in Fig. 3. The consistency between data of P and R branches indicates excellent quality of our data and accurate calibration of our instrumental re-

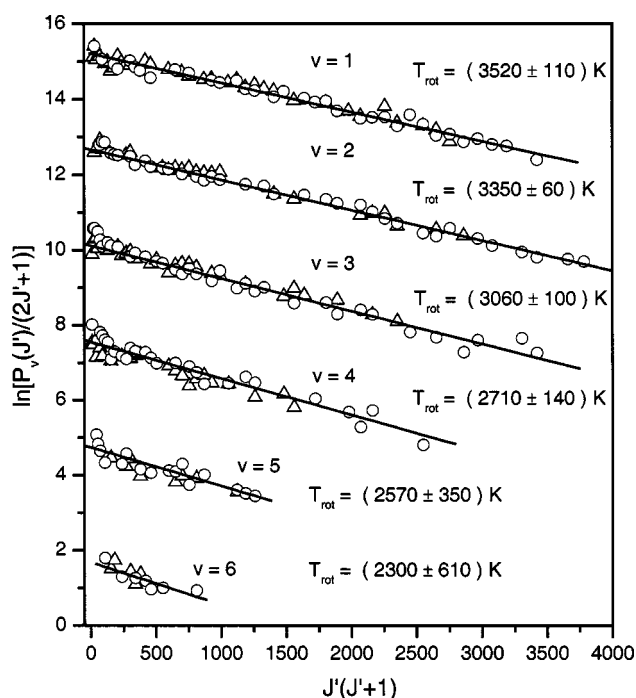


FIG. 3. Semilogarithmic plots of relative rotational populations of $\text{CO}(v=1-6)$ upon photolysis of $(\text{CICO})_2$ at 193 nm. Symbols Δ are from P lines and \circ are from R lines. Solid lines represent least-squares fits; rotational temperatures are listed.

sponse function. Deduced rotational temperatures are 3520 ± 110 , 3350 ± 60 , 3060 ± 100 , 2710 ± 140 , 2570 ± 350 , and 2300 ± 610 K for $v=1-6$, respectively. The rotational temperature of $\text{CO}(v=1)$ is ~ 1.5 times that observed upon photolysis of $(\text{CICO})_2$ at 248 nm. Rotational energies $E_{\text{rot}}(v)$ for each vibrational level, obtained on summing a product of level energy and normalized population of each rotational level, are listed in Table I. A sum of relative rotational population in each vibrational state is listed in column $\sum J P_v(J)$ of Table I; the ratio gives a relative vibrational population. A rotational energy of 22.8 kJ mol^{-1} averaged over $v=1-6$ is derived on multiplying $E_{\text{rot}}(v)$ from observed data by its corresponding relative vibrational population, to be discussed later.

Energetically, with a maximal energy $\sim 14\,039 \text{ cm}^{-1}$ of vibration–rotational excitation observed for $\text{CO}(v=6, J=29)$, the $v=7$ level is expected to be populated up to $J=4$, but we are unable to identify positively these lines because their intensities are small and because other lines overlap. An energy limit of $14\,039 \text{ cm}^{-1}$ corresponds to levels up to $J=79, 72, 64, 54, 43$ for $v=1-5$, respectively. We observed J values up to 60, 61, 58, 50, and 40 for $v=1-5$; hence unobserved lines due to lack of sensitivity has only a small effect on the calculation of average rotational energy, especially when the kinematic constraints for rotational distributions are taken into consideration. Considering possible experimental errors including possible neglect of weak lines, we report an average rotational energy of $23 \pm 3 \text{ kJ mol}^{-1}$ for

TABLE I. Rotational temperature (T_{rot}), rotational energy (E_{rot}), and vibrational population of $\text{CO}(v)$ upon photolysis of $(\text{CICO})_2$ at 193 nm.

| v | T_{rot}/K | $\sum J P_v(J)^a$ | $E_{\text{rot}}/\text{kJ mol}^{-1}$ | Rel. population |
|-----|---------------------------|-------------------|-------------------------------------|--------------------|
| 0 | | | | 0.460 ^b |
| 1 | 3520 ± 110 | 36 717 | 24.3 | 0.258 |
| 2 | 3350 ± 60 | 20 821 | 23.8 | 0.146 |
| 3 | 3060 ± 100 | 11 052 | 21.6 | 0.078 |
| 4 | 2710 ± 140 | 5449 | 17.7 | 0.038 |
| 5 | 2570 ± 350 | 2051 | 13.4 | 0.014 |
| 6 | 2300 ± 610 | 822 | 8.10 | 0.006 |

^a $P_v(J)$ =(relative integrated emittance)/[(instrumental response factor)(Einstein coefficient)]; arbitrary unit.

^bEstimated from surprisal analysis.

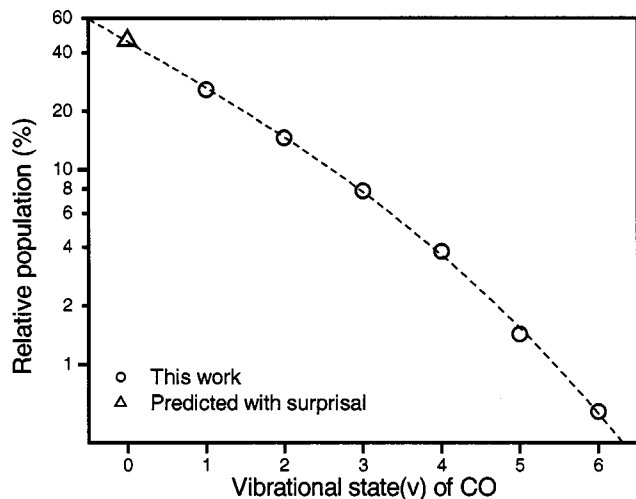


FIG. 4. Vibrational distribution of CO upon photolysis of $(\text{ClCO})_2$ at 193 nm. Population of $v=0$ (Δ) is estimated with a surprisal analysis.

CO observed in this work. This value is $\sim 43\%$ greater than the value of $16 \pm 2 \text{ kJ mol}^{-1}$ derived for photolysis of $(\text{ClCO})_2$ at 248 nm.²

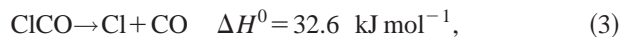
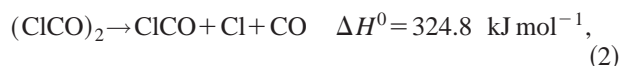
B. Vibrational distribution of CO

The ratio of $\sum_J P_v(J)$ in Table I yields a relative vibrational population for $\text{CO}(v=1-6)$. Based on this observed vibrational distribution, we estimate by surprisal analysis the population of $v=0$ relative to that of $v=1$ to be 1.78 ± 0.17 ; the small population of $v=7$ may be neglected. The vibrational distribution of CO normalized for $v=0-6$ is shown in Table I and Fig. 4. The average vibrational energy of CO thus derived is 26.0 kJ mol^{-1} . Considering possible errors including that in estimating population of $\text{CO}(v=0)$, we report an average vibrational energy of $26 \pm 4 \text{ kJ mol}^{-1}$ for CO observed in this work; this value is 2.6 times the value of $10 \pm 3 \text{ kJ mol}^{-1}$ observed for photolysis at 248 nm.

Hemmi and Suits⁴ were unable to resolve the vibrational distribution in their photofragment translational spectra of CO; the observed translational energy of CO has an average $\sim 41.7 \text{ kJ mol}^{-1}$ and extends to $\sim 85 \text{ kJ mol}^{-1}$. The average internal energy of CO, 49 kJ mol^{-1} , observed in this work is consistent with their observations.

C. Energy balance and mechanism of photodissociation

Standard enthalpies of reaction at 298 K for the following channels are:



according to standard enthalpies of formation: $-335.8 \pm 6.3 \text{ kJ mol}^{-1}$ for $(\text{ClCO})_2$,⁸ $-21.8 \pm 2.5 \text{ kJ mol}^{-1}$ for ClCO ,⁹ $121.3 \text{ kJ mol}^{-1}$ for Cl , and $-110.53 \text{ kJ mol}^{-1}$ for CO .¹⁰ At 0 K, enthalpies of reaction are 289.0, 318.3, and

29.2 kJ mol^{-1} for reactions (1)–(3), respectively. Because of uncertainties in enthalpies of formation for $(\text{ClCO})_2$ and ClCO , ΔH^0 of reactions (1) and (2) may have errors as large as 9 kJ mol^{-1} .

Ahmed *et al.*³ proposed that, on photolysis at 235 nm, $(\text{ClCO})_2$ undergoes an impulsive three-body dissociation [reaction (2)] to form translationally rapid Cl and CO, and translationally slow ClCO, followed by further decomposition of internally excited ClCO into Cl and CO. We derived a revised energy balance for photodissociation of $(\text{ClCO})_2$ at 248 nm that is consistent with the mechanism of three-body dissociation. Because our experiments were performed in a flow system at 298 K, thermal energies of reactants were taken into account in the energy balance. After breakage of C–C and C–Cl bonds in an initial three-body dissociation at 248 nm (482 kJ mol^{-1}), with average kinetic energies of Cl and CO determined to be 47.2 and 30.3 kJ mol^{-1} ,³ respectively, and the internal energy of CO to be 26 kJ mol^{-1} ,² the average internal energy of ClCO before further decomposition is about 64 kJ mol^{-1} ; the energy balance is listed in detail in Table II of Ref. 2. ClCO with such internal energy is unstable because breakage of its C–Cl bond requires only 32.6 kJ mol^{-1} . After secondary dissociation of ClCO, with observed translational energies of Cl and CO,³ the energy balance leaves about 10 kJ mol^{-1} for the average internal energy of the slow CO, too small to populate substantially the $v=1$ level, but consistent with the rotational distribution of $\text{CO}(v=0)$ previously observed with REMPI; in the REMPI experiments translationally slow CO was observed at $v=0$, $J=22$ ($E=11.6 \text{ kJ mol}^{-1}$).³ The infrared emission of CO that we observed results only from translationally rapid CO molecules produced in the initial step, not from cold CO produced from secondary dissociation.

We have identified an absorption band near 1880 cm^{-1} ascribable to the C–O stretching (v_1) mode of ClCO produced from reaction of $\text{Cl} + \text{CO}$ in our previous work,¹¹ but we observed no emission of ClCO upon photolysis of $(\text{ClCO})_2$ at 248 or 193 nm, indicating that either $\text{ClCO}(v_1=1)$ decomposes rapidly or that little $\text{ClCO}(v_1=1)$ was produced. Most surviving ClCO is expected to have an internal energy smaller than the C–Cl bond energy of 32.6 kJ mol^{-1} . This energy is sufficient to populate $v_1=1$ level ($\sim 22 \text{ kJ mol}^{-1}$) of the C–O stretching mode, but most of the vibrational excitation is likely associated with low-energy C–Cl stretching or ClCO-bending modes rather than with C–O stretching motion. The two small vibrational wave numbers, calculated to be 581 and 340 cm^{-1} ,^{11,12} lie beyond our detection limits.

If the same three-body dissociation mechanism proposed for photolysis of $(\text{ClCO})_2$ at 248 nm were used for photolysis at 193 nm, available energies for the fragments are 295 kJ mol^{-1} when the total bond-breaking energy for the reaction



is substrated from the available energy. The average translational energies of CO and Cl determined previously for the translationally rapid components are 41.7 and 46.0 kJ mol^{-1} ,

TABLE II. Energy balance (in kJ mol^{-1}) on photolysis of $(\text{ClCO})_2$ at 193 nm.

| Description | Energy | Adjustment for thermal energy ^a | Balance |
|---|---------|--|---------|
| Production of rapid Cl and CO | | | |
| photoexcitation energy | 619.2 | | 619.2 |
| fission of C–C and two C–Cl bonds, reaction (4) | –357.4 | | 261.8 |
| E_{trans} of rapid Cl (Ref. 4) | –46.0×2 | +3.7×2 | 177.2 |
| E_{trans} of rapid CO (Ref. 4) | –41.7×2 | +3.7×2 | 101.2 |
| E_{rot} of rapid CO (this work) | –23×2 | +2.5×2 | 60.2 |
| E_v of rapid CO ($v \leq 6$) (this work) | –26×2 | +0.0 | 8.2 |
| Production of slow Cl and CO | | | |
| photoexcitation energy | 619.2 | | 619.2 |
| fission of C–C, reaction (1) | –292.2 | | 327.0 |
| electronic excitation of one ClCO | –210 | | 117 |
| energy of each ClCO | 58.5 | | |
| fission of one C–Cl bond, reaction (3) | –32.6 | | 25.9 |
| E_{trans} of slow Cl (Ref. 4) | –14.5 | +3.7 | 15.1 |
| E_{trans} of slow CO (Ref. 4) | –10.7 | +3.7 | 8.1 |
| E_v of slow CO ^b | –0 | +0.0 | 8.1 |
| E_{rot} of slow CO ^b | –10 | +2.5 | 0.6 |

^aBecause available enthalpies of reaction are at 298 K, thermal energies of reactants and products need to be taken into account; see text.

^bAssuming that the internal distribution of slow CO is similar to that produced at 235 nm (Ref. 3).

respectively,⁴ and the internal energy of CO is determined in this work to be 49 kJ mol^{-1} . The spin–orbit components $\text{Cl}(^2P_{3/2})$ and $\text{Cl}(^2P_{1/2})$ could not be distinguished in experiments using photofragment translational spectroscopy; the observed energy should be consequently considered an average for both spin–orbit components. The energy balance implies that ClCO would have internal energy of $\sim 163 \text{ kJ mol}^{-1}$ if the average translational energy of ClCO is $\sim 5 \text{ kJ mol}^{-1}$.⁴ With such a large internal energy, ClCO is expected to further decompose into Cl and CO. Taking into account previously observed average kinetic energies of slow Cl and CO, 14.5 and 10.7 kJ mol^{-1} , respectively, and the bond energy for Cl–CO, 32.6 kJ mol^{-1} , CO should have average internal energy of $\sim 113 \text{ kJ mol}^{-1}$, much greater than our observation of 49 kJ mol^{-1} . For the survived ClCO, an average translational energy of 4.6 kJ mol^{-1} and a maximum energy of $\sim 10 \text{ kJ mol}^{-1}$ was reported previously;⁴ its internal energy should be less than 32.6 kJ mol^{-1} unless it is metastable.

The only possibility to balance the energy is to assume that both CO fragments have large translational and internal energies and both Cl fragments also have large translational energy. With an excitation energy of 619 kJ mol^{-1} , available energies for the fragments are 262 kJ mol^{-1} when the total bond-breaking energy for the reaction



is subtracted from the available energy. With average translational energies of 41.7 and 46.0 kJ mol^{-1} , respectively,⁴ determined previously for the translationally rapid components of CO and Cl, and the internal energy of CO of 49 kJ mol^{-1} determined in this work, the total energy of 273 kJ mol^{-1} for two pairs of Cl and CO hence matches satisfactorily the available energy when thermal energies of products are taken into account. A detailed balance in energy is listed in Table II.

Because in our experiments we are unable to distinguish a small variation in distributions of rotational energy of these two CO fragments, the energy balance does not require that both CO fragments have identical internal energies, but the absence of an evident bimodal rotational distribution indicates that both CO fragments have similar internal energies. The most likely mechanism for formation of rapid components of CO and Cl is hence a four-body dissociation with one C–C and two C–Cl bonds breaking at nearly the same time. A mechanism of sequential decomposition proposed for photodissociation at 248 nm is unlikely to be applicable also at 193 nm because of energy balance and because a different vibrational and rotational distribution would be expected for CO and Cl produced in different steps. The anisotropy of these rapid fragments is high, with $\beta = 0.8$ for Cl and 0.4 for CO.⁴ Preliminary experiments on decomposition of $(\text{ClCO})_2$ at 193 nm with REMPI detection of Cl and CO using femtosecond laser beams indicate that Cl and CO are produced promptly, within their instrument response time of $\sim 100 \text{ fs}$.¹³

We employed time-dependent density-functional theory (TD-DFT) to predict vertical excitations of $(\text{ClCO})_2$ and found two major transitions at 5.39 and 6.72 eV , corresponding to ~ 230 and $\sim 184 \text{ nm}$. The former corresponds to excitation to the 1^1B_u state that is associated mainly with excitation from a nonbonding Cl orbital (ϕ_{27}) to an orbital (ϕ_{32}), described approximately as a π orbital bonding between C–C but anti-bonding within each C–O and C–Cl bond. The latter corresponds to excitation to the 2^1B_u state that is associated mainly with excitation from the highest occupied molecular orbital (ϕ_{31}) to an orbital (ϕ_{33}) described approximately as a σ orbital antibonding within all C–C, C–O, and C–Cl bonds. This surface is hence likely to be responsible for prompt cleavage of all C–C and C–Cl bonds upon excitation at 193 nm.

Hemmi and Suits⁴ observed also components of Cl and CO with small translational energy which they ascribed to be produced via secondary decomposition of CICO. As described previously, the CICO fragments would have a total energy of 167 kJ mol⁻¹ after the initial decomposition step in the three-body decomposition model. Such a large energy is inconsistent with observed translational energies of 14.5 and 10.7 kJ mol⁻¹ for slow Cl and CO, and a maximal internal energy of 49 kJ mol⁻¹ for CO; at least 70 kJ mol⁻¹ energy is unaccounted. The discrepancy in energy balance might be as much as 109 kJ mol⁻¹ if the CO fragment produced in the secondary dissociation has little (~ 10 kJ mol⁻¹) internal energy so that its IR emission is absent, as in the case of photolysis at 248 nm. Such a large discrepancy cannot be attributed to errors in measurements of internal energies of fragments and in analysis of photofragment translational spectra arising from difficulties in accurate momentum matching in the three-body dissociation. In the extreme case in which both pairs of CO and Cl are translationally slow and CO has little internal energy, the discrepancy in energy is $\sim 619.2 - 357.4 - 2 \times (14.5 + 10.7 + 10) + 2 \times (3.7 + 3.7 + 2.5) = 211$ kJ mol⁻¹.

Possible mechanisms to account for this energy difference include radiation of electronically excited (CICO)₂ to a lower electronic state and formation of electronically excited CICO (denoted CICO* hereafter) or ClC₂O₂ (denoted ClC₂O₂*) that emits. Electronic states of (CICO)₂ and ClC₂O₂ are little investigated, either experimentally or theoretically, but emission from electronically excited (CICO)₂ can not compete with rapid four-body dissociation.

Krossner *et al.*¹⁴ carried out MRD-CI calculations to predict the first two vertical electronic excitations of CICO to be ~ 312 and 323 kJ mol⁻¹ for excitation to ²A'' and ²A' states, respectively. Francisco and Goldstein¹⁵ employed unrestricted second-order Møller–Plesset perturbation theory (UMP2 and PUMP/6-31G*) to predict an A ²Σ⁺ state lying ~ 4 kJ mol⁻¹ and a B ²Π(A'') state lying ~ 218 kJ mol⁻¹ above the ground X ²A' state of CICO; the latter matches satisfactorily with the energy deficiency of 211 kJ mol⁻¹ derived previously when two pairs of translationally slow Cl and CO (also internally cold) are produced. Hence, a possible mechanism would be production of CICO and CICO* upon excitation at 193 nm, followed by emission from CICO*; a fraction of CICO might decompose to form cold Cl and CO. Given an electronic excitation ~ 210 kJ mol⁻¹ for CICO, the energy balance implies that, after breaking the C–C bond, CICO and CICO* each has an energy ~ 58.5 kJ mol⁻¹; with this energy, a proportion of CICO decomposes to form translationally slow Cl and CO with energies consistent with experimental observation of photofragment translational spectroscopy. A detailed balance is listed in the second part of Table II; the internal energy of ~ 10 kJ mol⁻¹ for the slow CO suggests that it is mainly in the $v=0$ state and undetectable in our system. The energy of CICO in this case is similar to that (64 kJ mol⁻¹) produced upon photolysis of (CICO)₂ at 248 nm, hence energies of secondary reaction products Cl and CO are similar in both cases. To understand fully the mechanism for formation of translationally

slow Cl and CO, further experiments and quantum-chemical calculations are needed.

In summary, the energy balance for photolysis of (CICO)₂ at 193 nm suggests that its mechanism of dissociation differ from that at 248 nm. At 248 nm, the initial step involves three-body decomposition of (CICO)₂ into translationally rapid Cl and CO ($v \leq 3$, $J \leq 50$) and CICO; a fraction of CICO further decomposes to form slow Cl and CO ($v=0$), which is undetectable with our technique. At 193 nm, a four-body dissociation with rapid fission of C–C and both C–Cl bonds produces two pairs of translationally rapid Cl and CO ($v \leq 6$, $J \leq 60$) with similar energies; the latter was observed in this work. Formation of translationally slow CICO, Cl, and CO reported previously⁴ might be rationalized with a second channel involving emission of electronically excited intermediates; CO produced in this mechanism might be mainly in the $v=0$ state and undetectable in this work.

IV. CONCLUSION

Rotationally resolved emission from CO up to $v=6$ and $J=60$ is observed upon photolysis of (CICO)₂ at 193 nm; the rotational distribution is Boltzmann, and average rotational and vibrational energies of CO are 23 ± 3 and 26 ± 4 kJ mol⁻¹, respectively. Our results combined with the distribution of translational energy determined with photofragment translational spectroscopy suggest the existence of a four-body dissociation channel producing one pair of translationally rapid Cl and one pair of translationally rapid and internally hot CO, with the latter having similar distributions of internal energy. Previously observed⁴ translationally slow CICO, Cl, and CO might result from a second channel involving emission of electronically excited intermediates; CO produced in this channel is expected to be mainly in the $v=0$ state, undetectable with TR-FTS method. We observed no emission of CICO near 1880 cm⁻¹, indicating that surviving CICO has little vibrational excitation in the C–O stretching mode.

ACKNOWLEDGMENTS

We thank the National Science Council of Taiwan (Grant No. NSC92-2113-M-007-034) and MOE Program for Promoting Academic Excellence of Universities (Grant No. 89-FA04-AA) for support.

¹A. V. Baklanov and L. N. Krasnoperov, J. Phys. Chem. A **105**, 97 (2001).

²C.-Y. Wu, Y.-P. Lee, J. F. Ogilvie, and N. S. Wang, J. Phys. Chem. A **107**, 2389 (2003).

³M. Ahmed, D. Blunt, D. Chen, and A. G. Suits, J. Chem. Phys. **106**, 7617 (1997).

⁴N. Hemmi and A. G. Suits, J. Phys. Chem. A **101**, 6633 (1997).

⁵P.-S. Yeh, G.-H. Leu, Y.-P. Lee, and I.-C. Chen, J. Chem. Phys. **103**, 4879 (1995).

⁶S.-R. Lin and Y.-P. Lee, J. Chem. Phys. **111**, 9233 (1999).

⁷J. F. Ogilvie, S.-L. Cheah, Y.-P. Lee, and S. P. A. Sauer, Theor. Chem. Acc. **108**, 85 (2002).

⁸L. C. Walker and H. Prophet, Trans. Faraday Soc. **63**, 879 (1967).

⁹J. M. Nicovich, K. D. Kreutter, and P. H. Wine, J. Chem. Phys. **92**, 3539 (1990).

¹⁰M. W. Chase, Jr., NIST-JANAF Thermochemical Tables, 4th ed., J. Phys. Chem. Ref. Data, Monograph **9** (1998).

¹¹S.-H. Chen, L.-K. Chu, Y.-J. Chen, I.-C. Chen, and Y.-P. Lee, *Chem. Phys. Lett.* **333**, 365 (2001).
¹²H. Schnöckel, R. A. Eberlein, and H. S. Plitt, *J. Chem. Phys.* **97**, 4 (1992).

¹³P.-Y. Cheng (unpublished).
¹⁴Th. Krossner, L. Zülicke, M. Staikova, and S.-D. Peyerimhoff, *Chem. Phys. Lett.* **241**, 511 (1995).
¹⁵J. S. Francisco and A. N. Goldstein, *Chem. Phys.* **128**, 367 (1988).